GGL: model-independent measurement of b/r

Idea:
Combine weak lensing and galaxy clustering to determine b and r.

- Galaxy clustering $\langle \delta_\mathrm{g}^2 \rangle$
- Galaxy-galaxy lensing, measures $\langle \delta_\mathrm{g} \delta \rangle$
- Cosmic shear, measures $\langle \delta^2 \rangle$

Cosmic shear is the most difficult to measure, so first measurements only used galaxy clustering and galaxy-galaxy lensing.

Form ratio:

$$\frac{\langle \delta_\mathrm{g} \delta \rangle(\theta)}{\langle \delta_\mathrm{g} \delta_\mathrm{g} \rangle(\theta)} = \frac{br}{b^2} = \frac{b}{r}.$$

Any cosmology-dependence, e.g. of clustering, drops out in the ratio.
These density correlations are projected to weak-lensing observables, and b and r (if constant) can directly be measured.

GGL: model-independent measurement of b and r I

Next: Combine all three

$$\langle \delta_{\rm g}^2 \rangle, \langle \delta_{\rm g} \delta \rangle, \langle \delta^2 \rangle.$$

to measure b and r.
Difficulty: Structure along all redshifts contribute to cosmic shear, not only mass associated with foreground galaxy sample $\delta_{\rm g}$.

Solutions:

- Choose background sample such that maximum lensing efficiency coincides with foreground redshift.
- Add correction functions with minor dependency on cosmology (geometry).

Redshift calibration factors

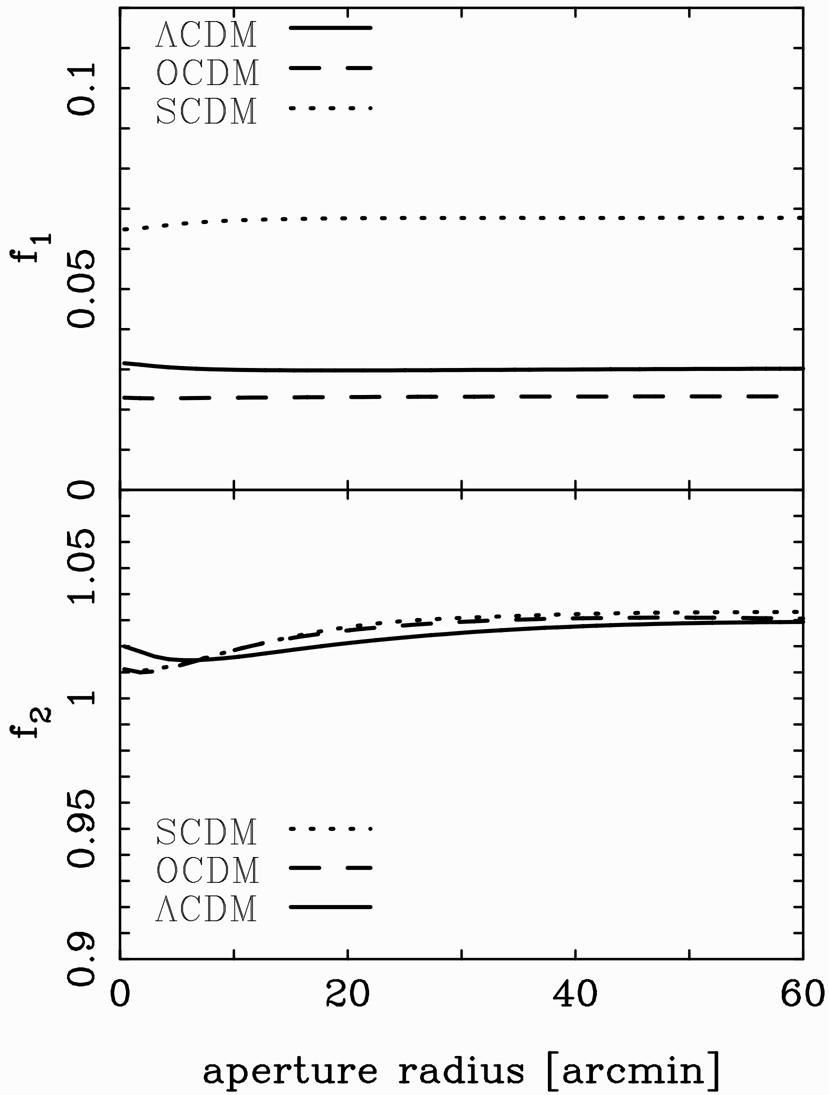

Scale-and cosmology-dependence of calibration factors. From (Simon et al. 2007), GaBoDS (Garching-Bonn Deep Survey).

GGL results: model-independent measurement of b/r

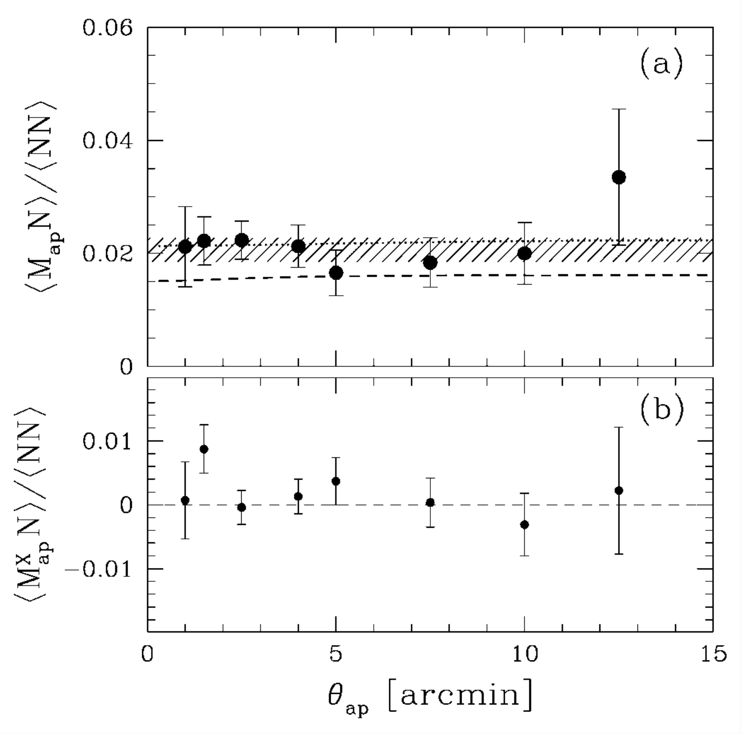

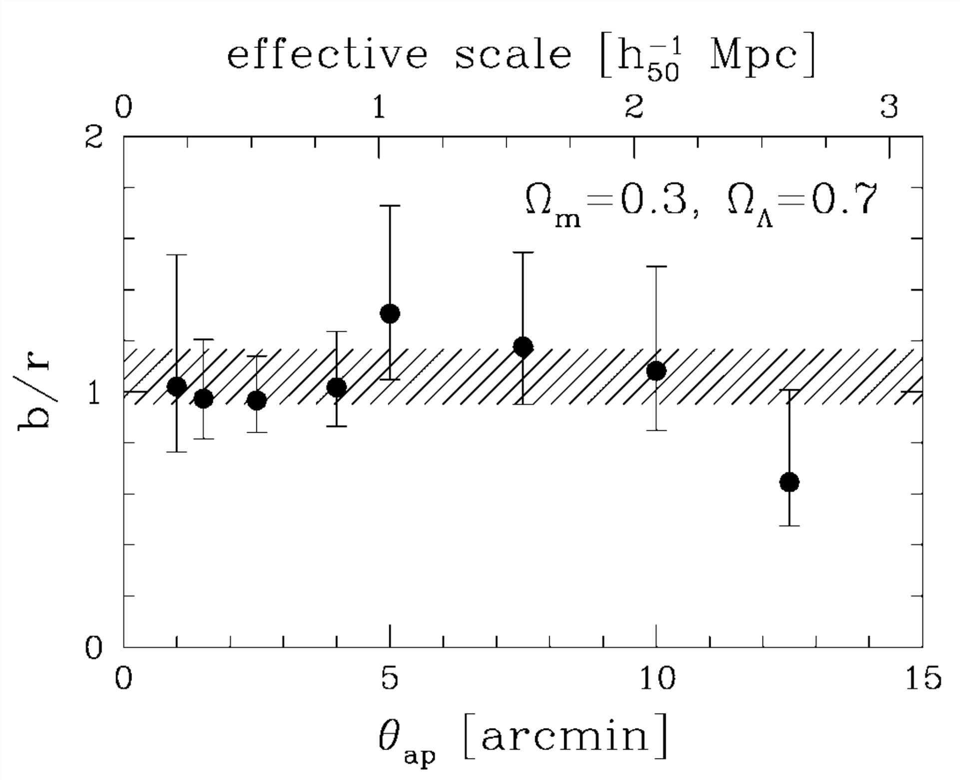

$$\mathcal{R} = \frac{r\Omega_m}{100b}[(5.8 - 1.6\Omega_m^{0.63}) + (4.6 - 2.6\Omega_m^{0.63})\Omega_\Lambda^{1.23}].$$

Observed ratio $\mathcal{R}$ (a), and B-mode (b); b/r (*right*) from (Hoekstra et al. 2001).

Main result: no scale-dependence found (on observed scales).

GGL results: model-indep. measurement of b and r I

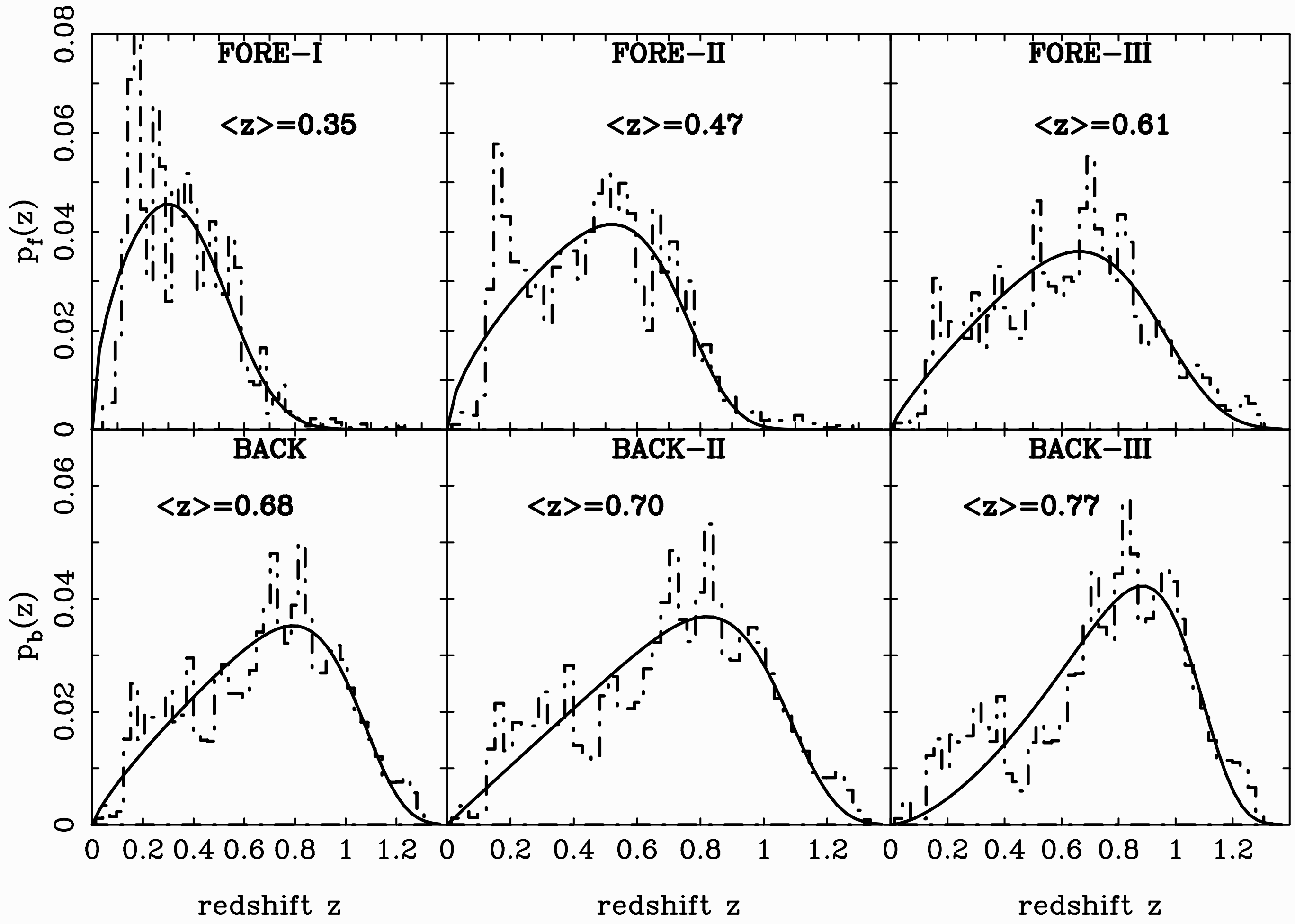

Redshift distributions for GaBoDS samples, estimated from COMBO-17. From (Simon et al. 2007), GaBoDS (Garching-Bonn Deep Survey).

GGL results: model-indep. measurement of b and r II

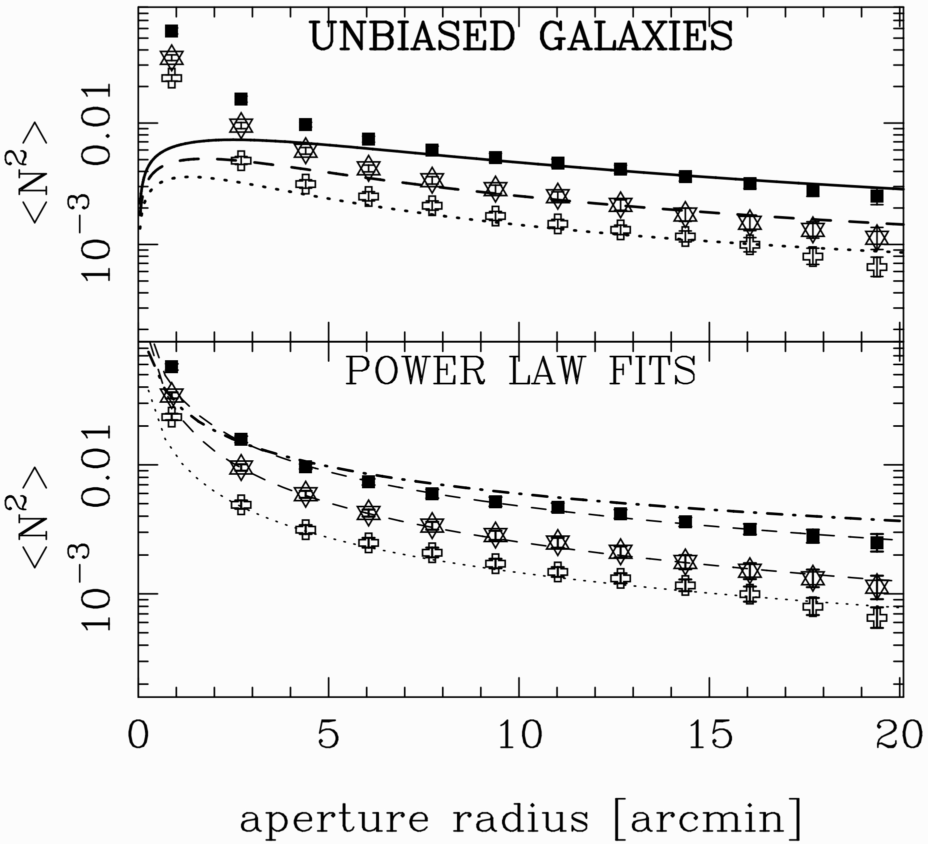

Filled boxes, open stars, open crosses = FORE-I, FORE-II, FORE-III.

Galaxy clustering: Bias on small scales is not constant, but scale-dependent. Stronger galaxy clustering than from constant bias. (Simon et al. 2007), GaBoDS (Garching-Bonn Deep Survey).

GGL results: model-indep. measurement of b and r III

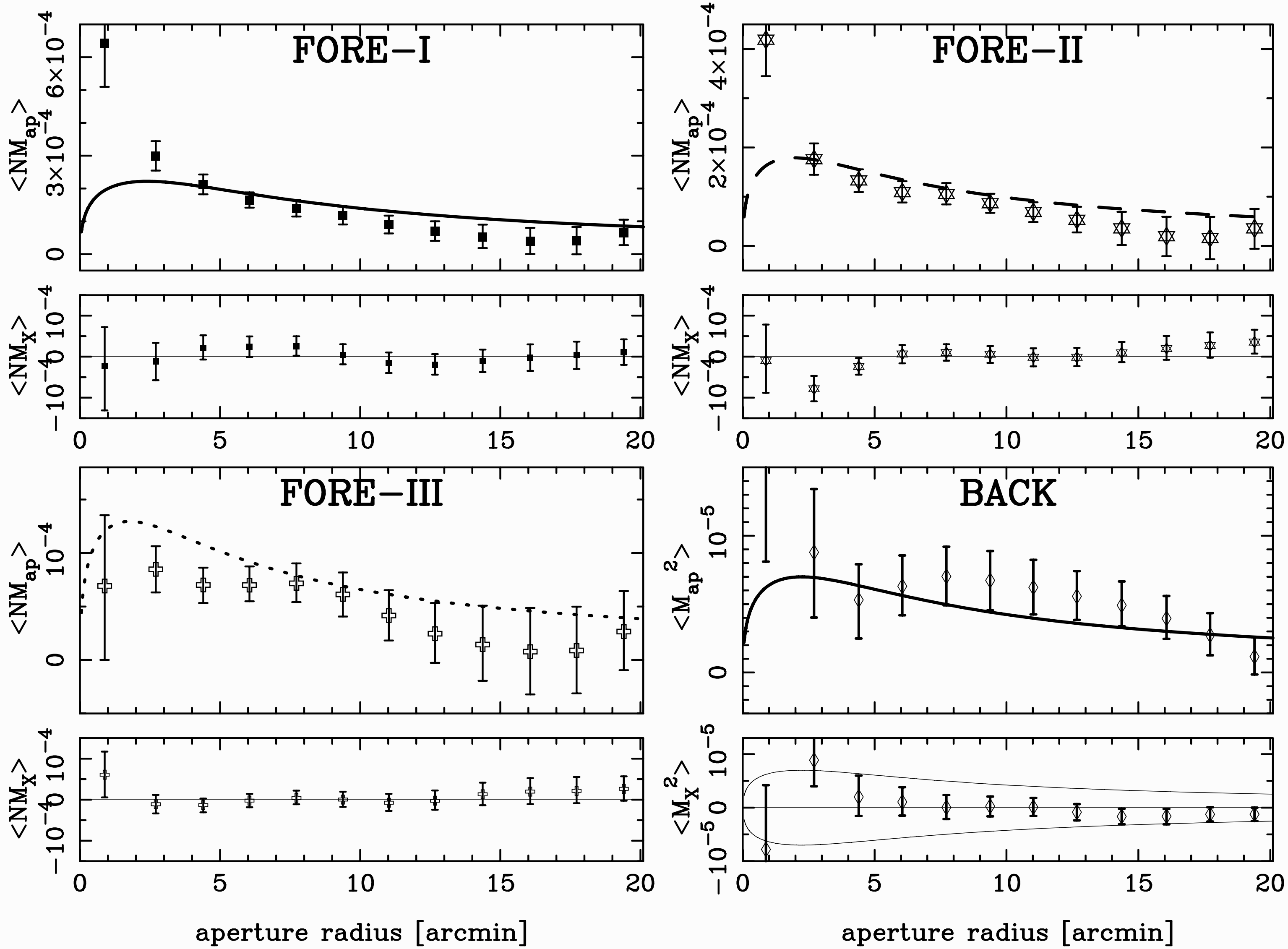

GGL and cosmic shear. (Simon et al. 2007), GaBoDS (Garching-Bonn Deep Survey).

GGL results: model-indep. measurement of b and r IV

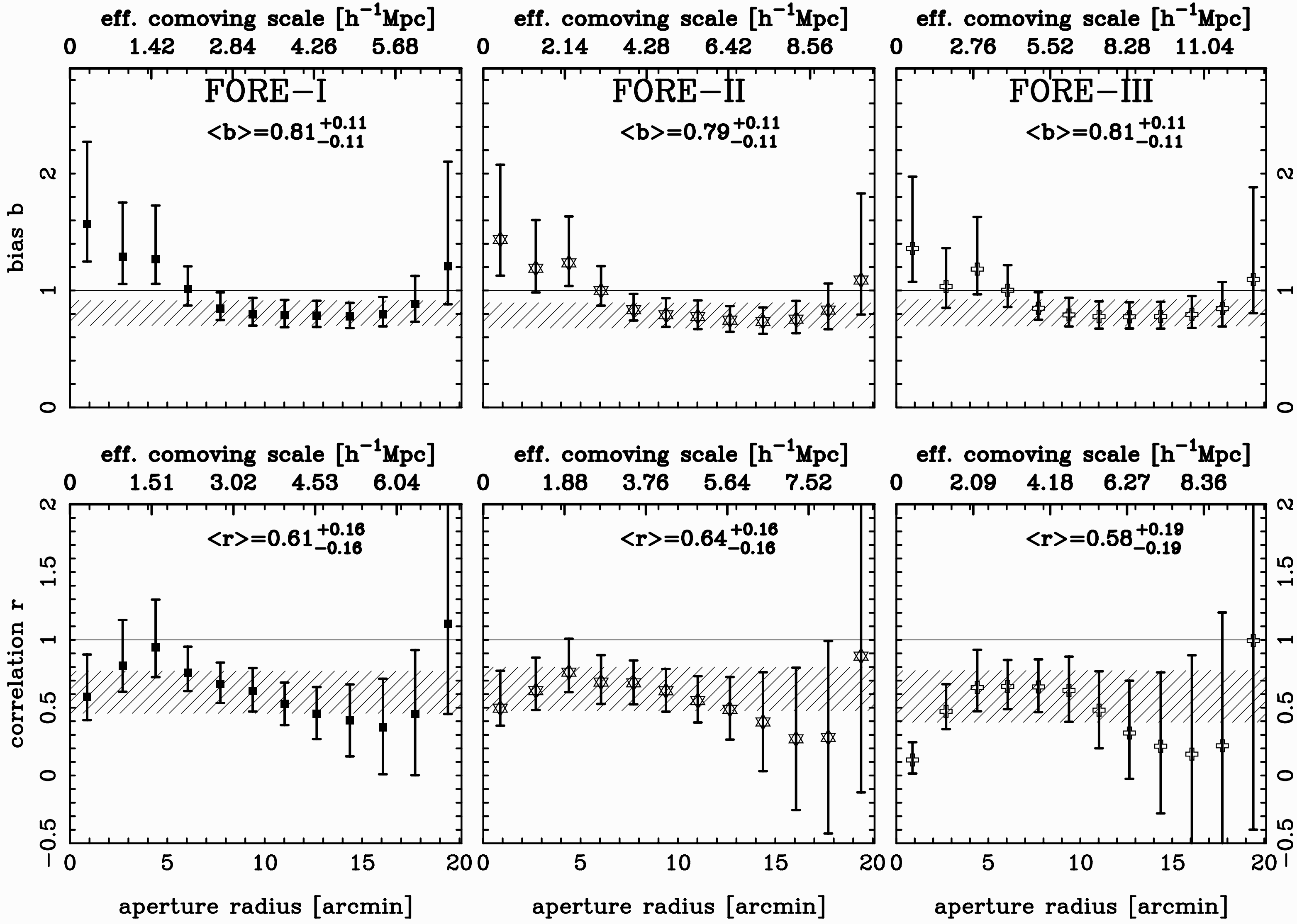

Bias and correlation coefficient. (Simon et al. 2007), GaBoDS (Garching-Bonn Deep Survey).

GGL: HOD model measurements

increasing luminosity →

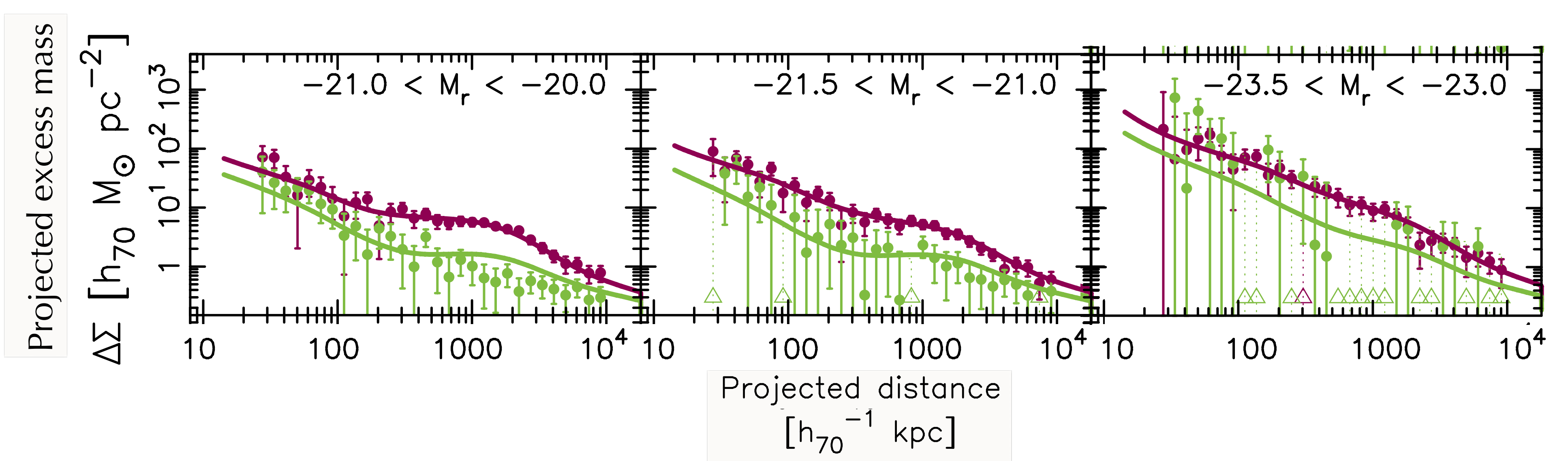

Purple=red early-type galaxies; Green=blue late-type galaxies. From (Velander et al. 2014).

GGL: HOD model measurements

increasing luminosity →

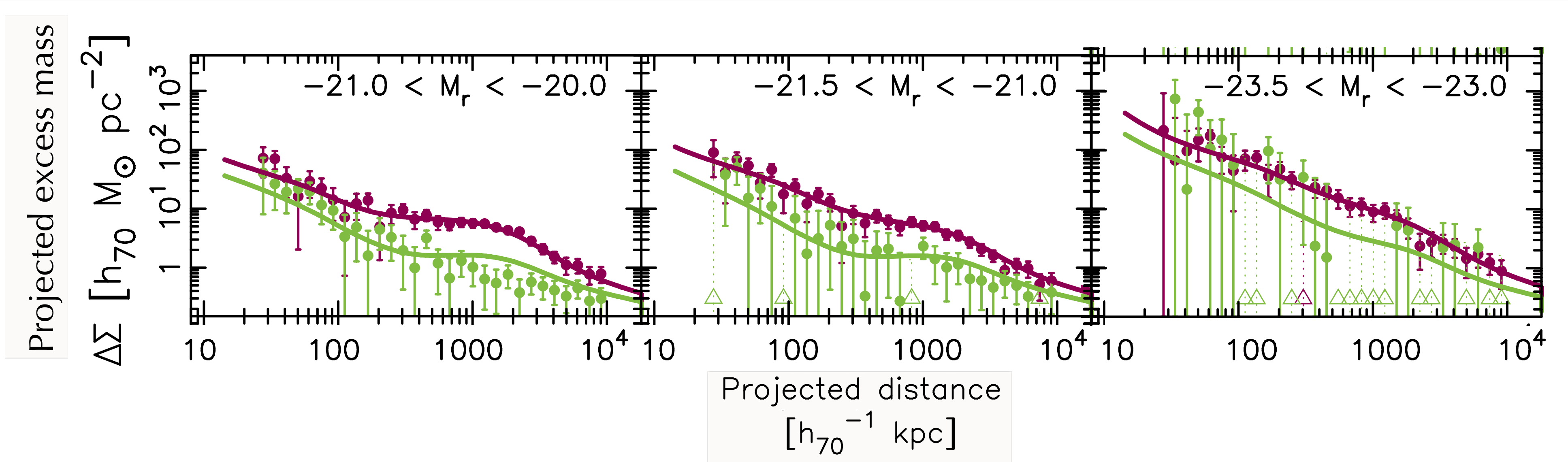

Purple=red early-type galaxies; Green=blue late-type galaxies. From (Velander et al. 2014).

- Red galaxies have larger associated mass than blue galaxies.
- Exceess mass increases with luminosity. Light traces mass.

GGL: HOD model measurements

increasing luminosity →

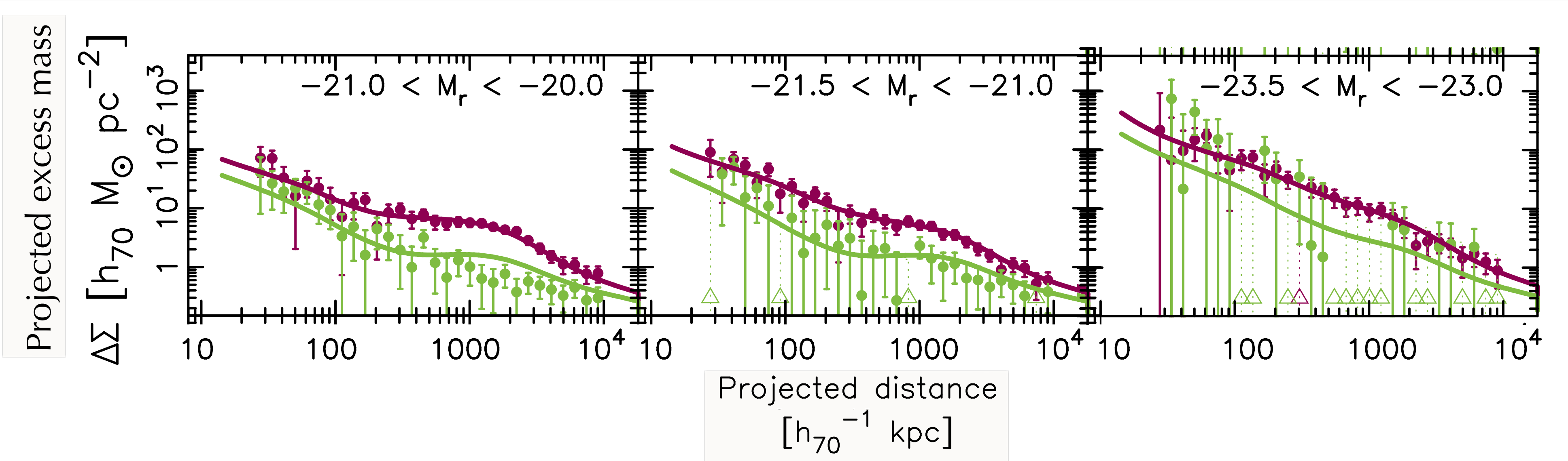

Purple=red early-type galaxies; Green=blue late-type galaxies. From (Velander et al. 2014).

- Red galaxies have larger associated mass than blue galaxies.
- Exceess mass increases with luminosity. Light traces mass.
- Bump at 1 Mpc for low-luminosity red galaxies, disappears at higher L. Red satellite galaxies.

GGL: HOD model measurements

increasing luminosity →

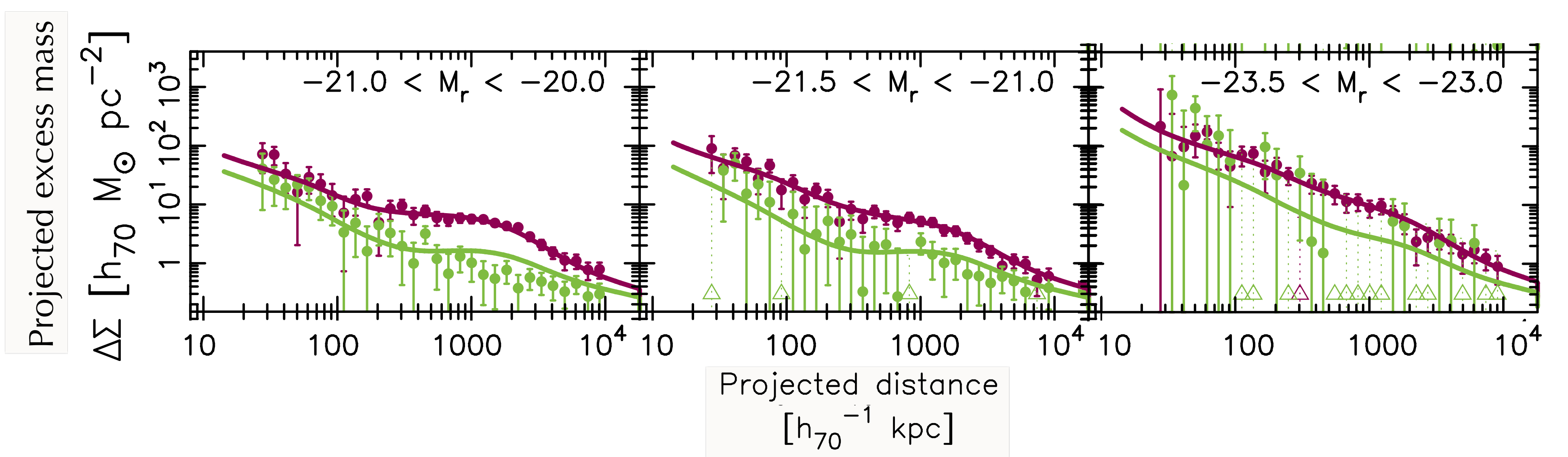

Purple=red early-type galaxies; Green=blue late-type galaxies. From (Velander et al. 2014).

- Red galaxies have larger associated mass than blue galaxies.
- Exceess mass increases with luminosity. Light traces mass.
- Bump at 1 Mpc for low-luminosity red galaxies, disappears at higher L. Red satellite galaxies.
- Bump at slightly larger scale for blue galaxies. 2-halo term, from clustered nearby galaxies.

GGL: HOD model

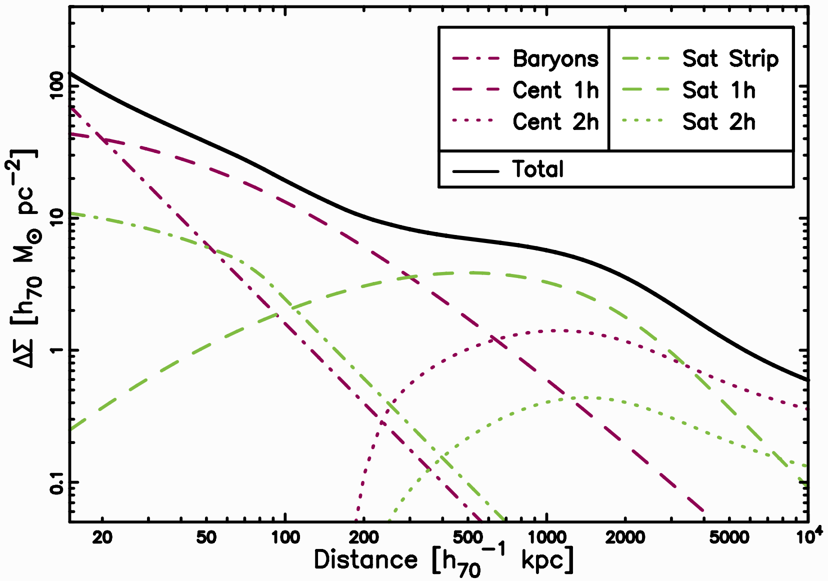

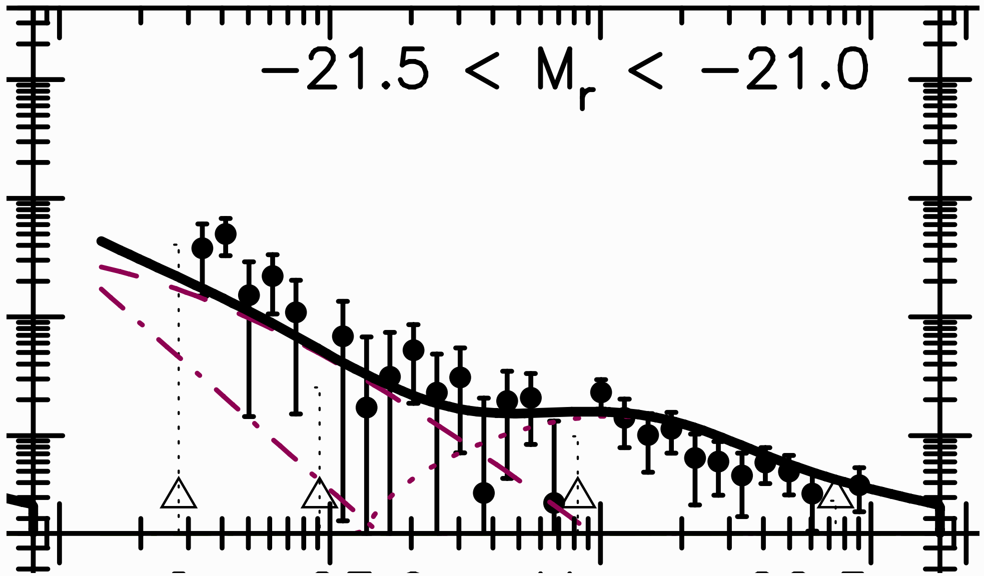

HOD model, (Velander et al. 2014).

GGL: M/L parameters

$$M_{200} = M_{0,L} \left(\frac{L}{L_{\rm fid}} \right)^{\beta_L}$$

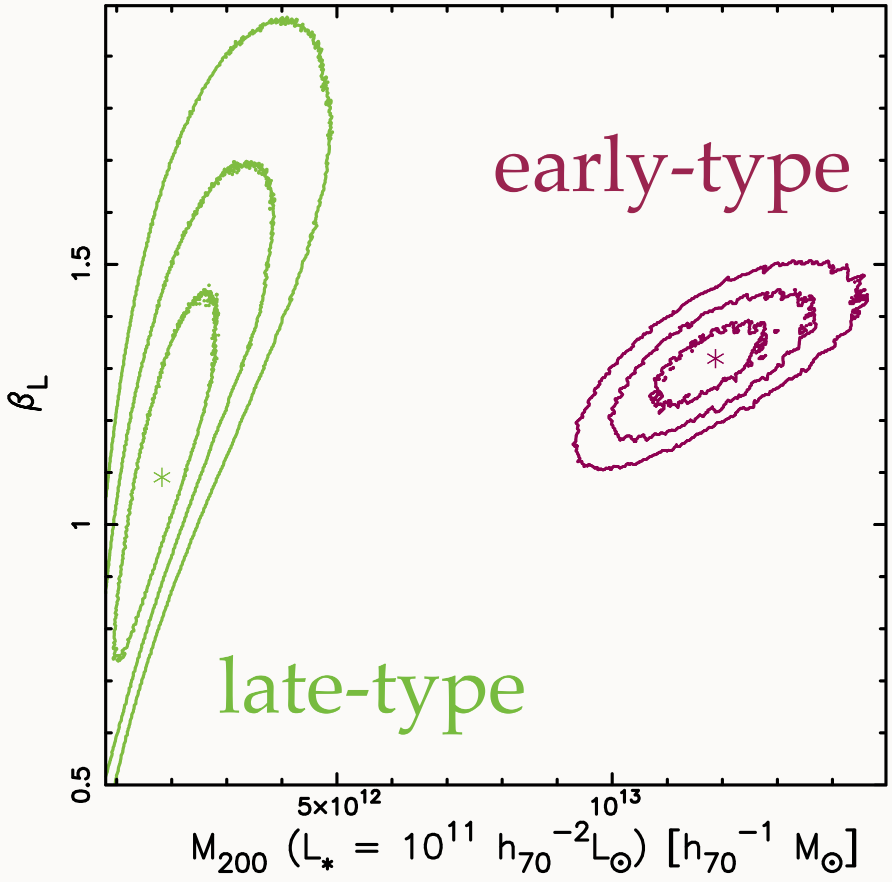

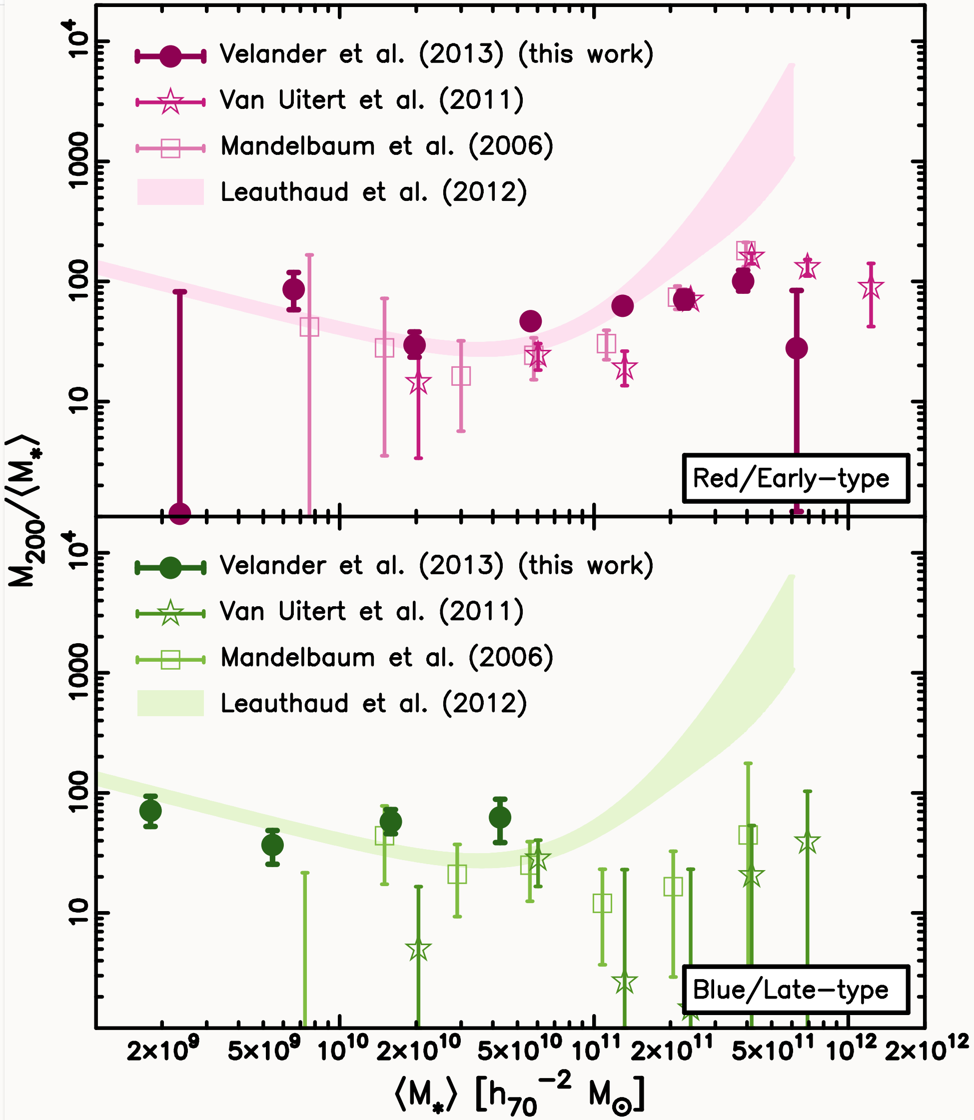

(Velander et al. 2014).

Modified gravity

General, perturbed Friedmann-Lemaître Robertson Walker (FLRW) metric:

$$\mathrm{d}s^2 = \left(1 + \frac{2\Psi}{c^2}\right) c^2 \mathrm{d}t^2 - a^2(t) \left(1 - \frac{2\Phi}{c^2}\right) \mathrm{d}l^2,$$

Valid for weak fields, (Bardeen) potentials $\Psi, \Phi \ll c^2$.

- In GR, and absence of anisotropic stress: $\Psi = \Phi$.
- In most modified gravity models: $\Psi \neq \Phi$! Very generic signature for MoG.

Some characteristics

- Ψ is Newtonian potential. Time-like. Quantifies time dilation.
- Ψ is gravitational action on non-relativistic objects (e.g. galaxies).
- Φ is space-like. Describes spatial curvature.
- $\Psi + \Phi$ is gravitational action on relativistic objects (e.g. photons; lensing!). [Photons travel equal parts of space and time. This is the origin for the factor two in GR equations compared to Newtonian mechanics!]

Testing GR I

Idea of a null test

Measure difference in potentials to test GR: Galaxy clustering for Ψ, weak lensing for $\Psi + \Phi$.

Modified Poisson equation

Potentials are related to density contrast δ via Poisson equation. Generalise to account for MoG, and write in Fourier space:

$$\begin{aligned} k^2 \tilde{\Psi}(k, a) &= 4\pi G a^2 \left[1 + \mu(k, a)\right] \rho \, \tilde{\delta}(k, a); \\ k^2 \left[\tilde{\Psi}(k, a) + \tilde{\Phi}(k, a)\right] &= 8\pi G a^2 \left[1 + \Sigma(k, a)\right] \rho \, \tilde{\delta}(k, a). \end{aligned}$$

With free parameters/functions μ, Σ. GR: $\mu = \Sigma = 0$.

Testing GR II

Probes of Bardeen potentials

Assuming linear, deterministic bias ($b =$const, $r = 1$).

- Galaxy clustering measures Ψ and b; $\langle \delta_{\rm g}^2 \rangle \propto b^2 P_\Psi$.
- GGL measures $\Psi + \Phi$ and b; $\langle \delta_{\rm g} \delta \rangle \propto b P_{\Psi+\Phi}$.

$\rightarrow$ form ratio to get rid of cosmology dependence!
However, bias still remains, need another observable.

- RSD anisotropy parameter; $\beta = \frac{1}{b} \frac{{\rm d} \ln D_+(a)}{{\rm d} \ln a}$.
  Can be measured from redshift space galaxy clustering along ($\mu = \cos\theta = 1$) and perpendicular ($\mu = 0$) to line of sight. Linear power spectrum:
  $$P(k, \mu) = P(k) \left(1 + \beta \mu^2\right)^2 .$$

$E_{\rm G}$ parameter

$$E_{\rm G} \simeq \frac{1}{\beta} \frac{\langle \delta_{\rm g} \delta \rangle}{\langle \delta_{\rm g}^2 \rangle}$$

Parenthesis: Anisotropic clustering

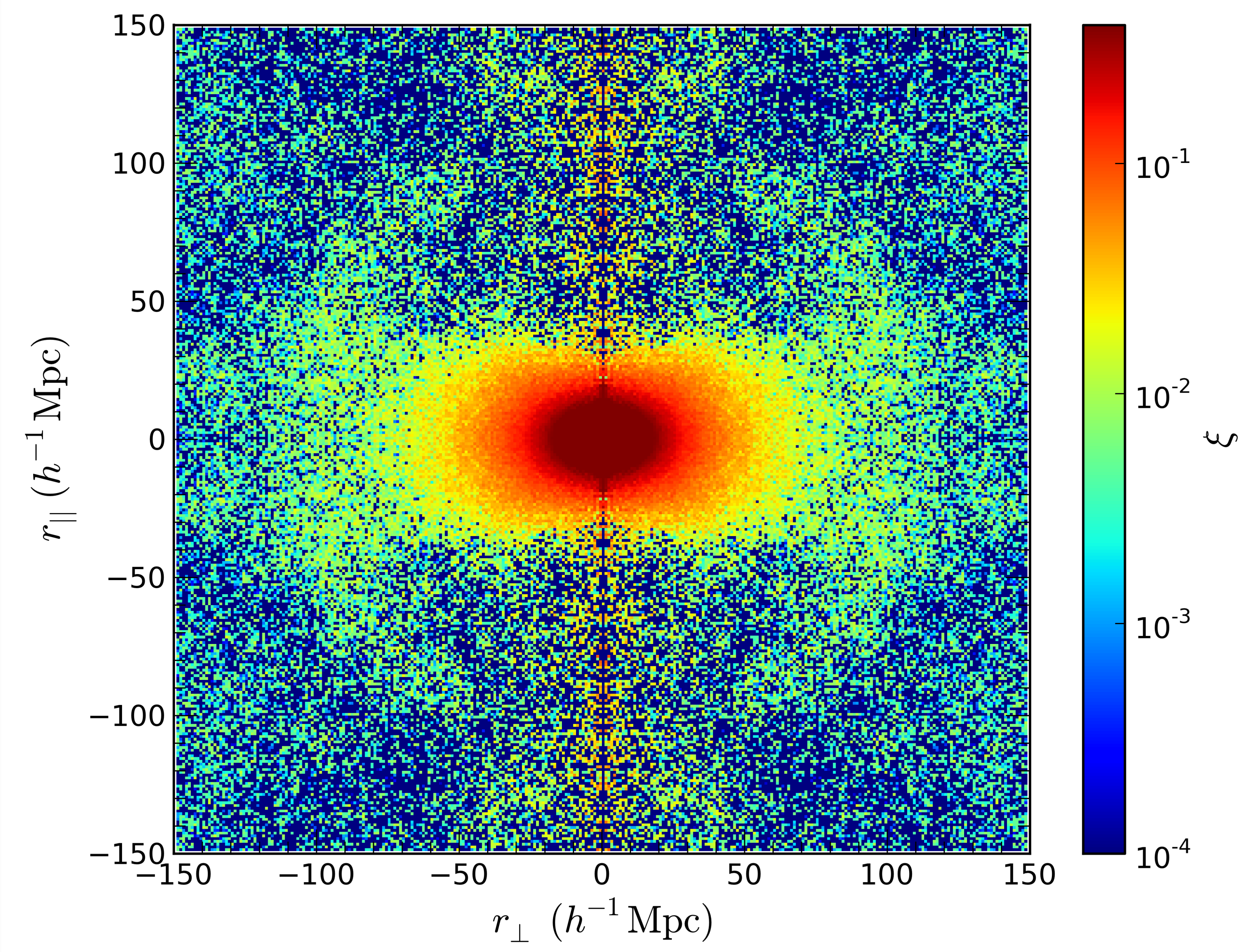

BOSS, from (Samushia et al. 2014).

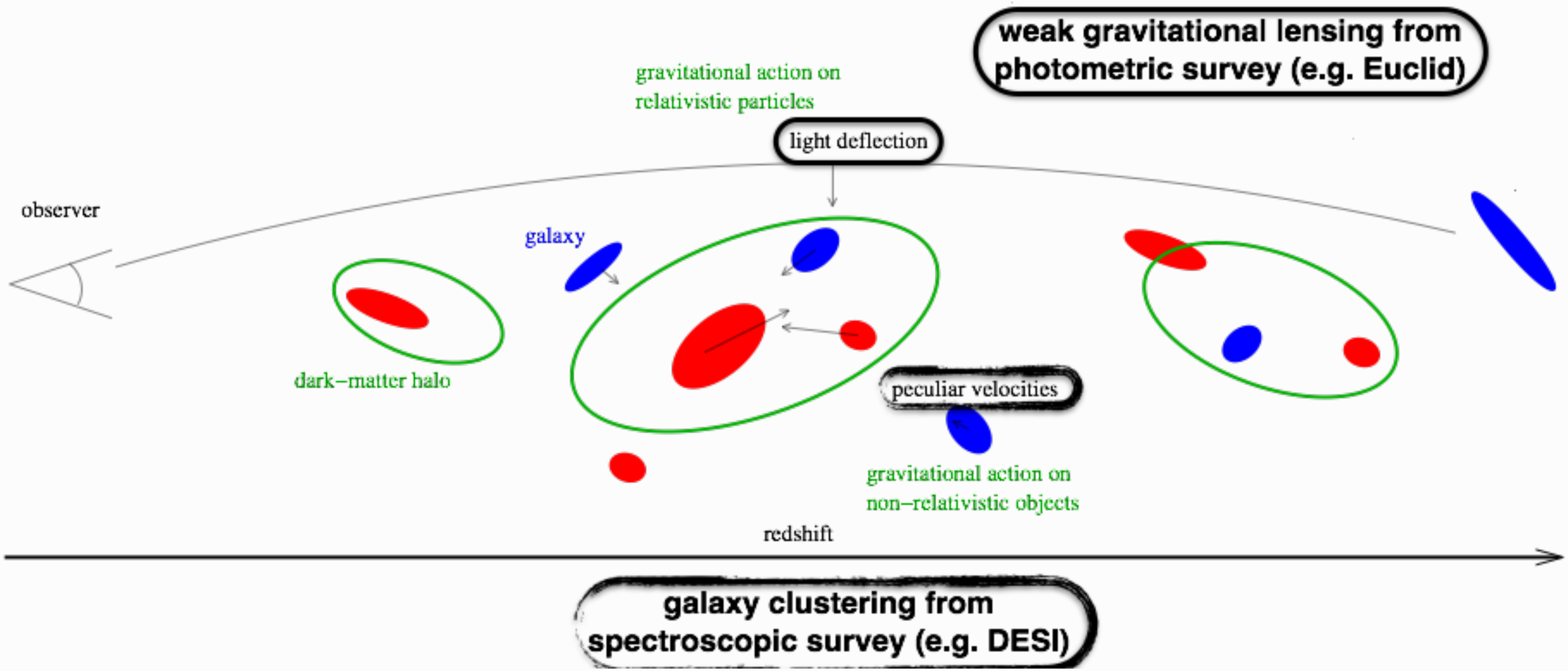
weak gravitational lensing from
photometric survey (e.g. Euclid)
gravitational action on
relativistic particles
light deflection
observer
galaxy
dark–matter halo
peculiar velocities
gravitational action on
non–relativistic objects
redshift
galaxy clustering from
spectroscopic survey (e.g. DESI)

Testing GR: results I

SDSS (Reyes et al. 2010)

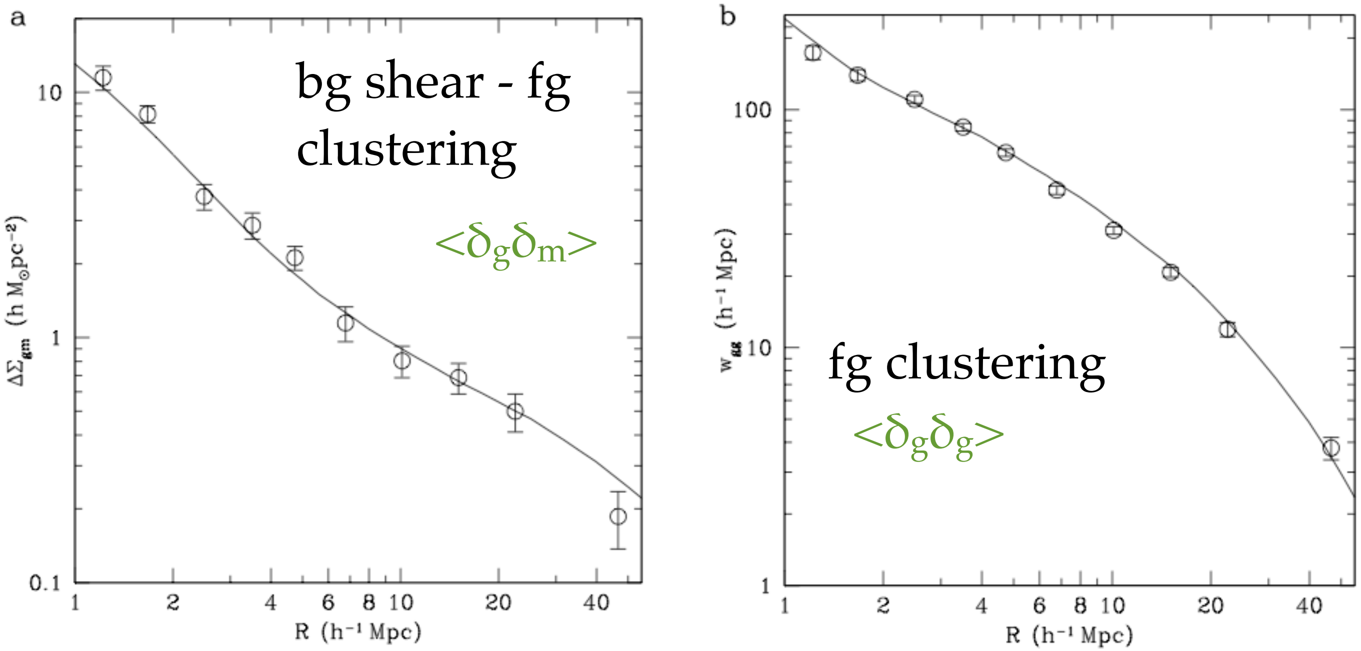

$\beta = 0.309 \pm 0.035$

from SDSS galaxy clustering (redshift-space distortions) Tegmark et al. (2006)

Testing GR: results II

Introducing new observable to exclude small scales:

$$\Upsilon_{\rm gm}(R) = \Delta\Sigma_{\rm gm}(R) - \left(\frac{R_0}{R}\right)^2 \Delta\Sigma_{\rm gm}(R_0)$$
$$= \frac{2}{R^2} \int_{R_0}^{R} {\rm d}R' \, R' \, \Sigma_{|rmgm}(R') - \Sigma_{\rm gm}(R') + \left(\frac{R_0}{R}\right)^2 \Sigma_{\rm gm}(R_0),$$

(Baldauf et al. 2010).

Define in analogy $\Sigma_{\rm gg}$.

Then modified $E_{\rm G}$ probe of gravity:

$$E_{\rm G}(R) = \frac{1}{\beta} \frac{\Sigma_{\rm gm}(R)}{\Sigma_{\rm gg}(R)}.$$

Testing GR: results III

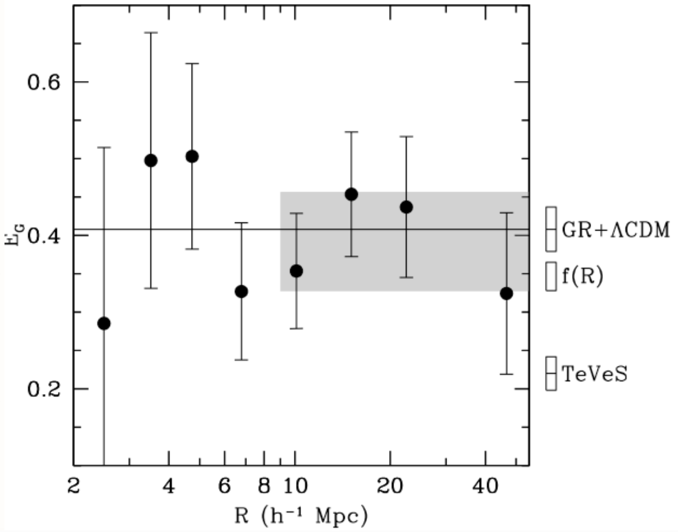

From (Reyes et al. 2010).

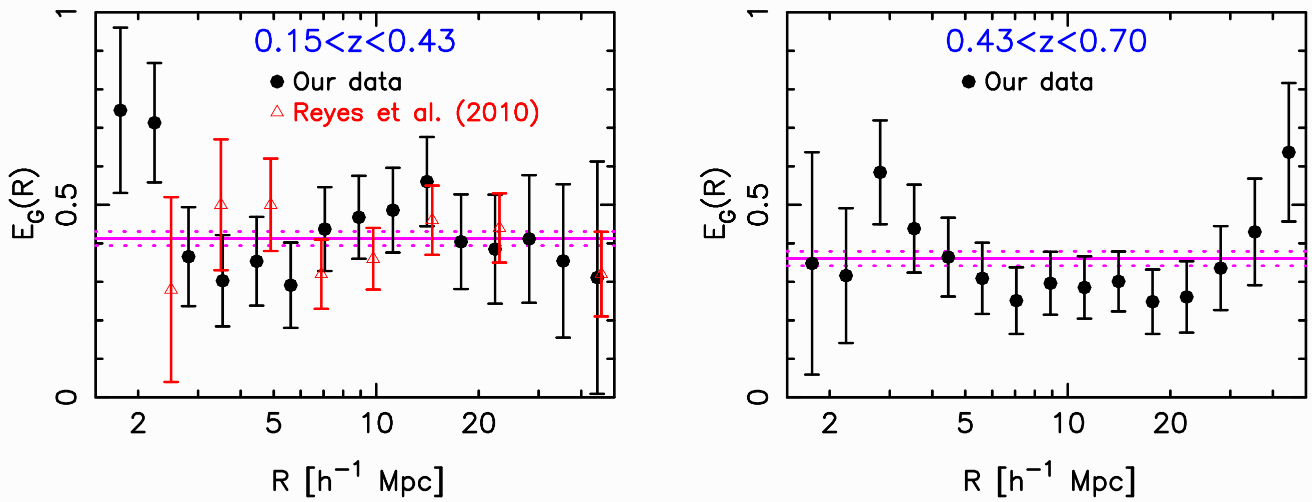

From (Blake et al. 2016).

E- and B-modes: recap I

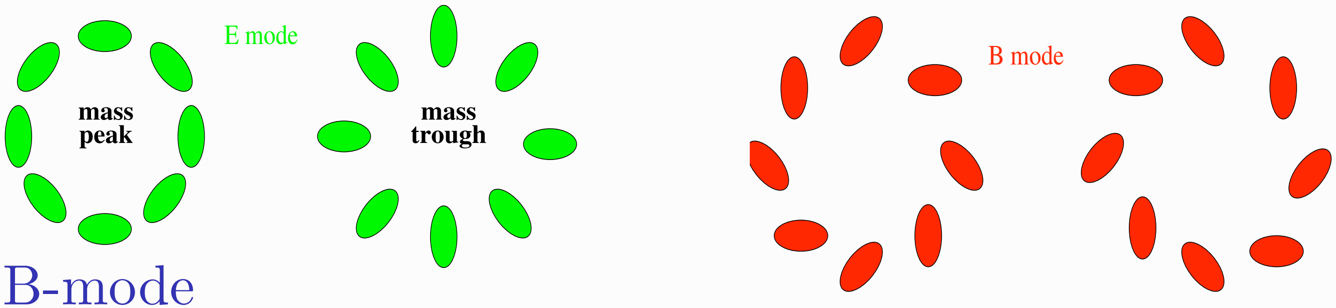

Origins of a B-mode

Measuring a non-zero B-mode in observations is usually seen as indicator of residual systematics in the data processing (e.g. PSF correction, astrometry).

Other origins of a B-mode are small, of %-level:

- Higher-order terms beyond Born appproximation (perturbed light rays, non-lin lens-lens coupling); other (e.g. some ellipticity estimators)
- Lens galaxy selection biases (size, magnitude biases), and galaxy clustering
- Intrinsic alignment (although magnitude not well-known!)
- Varying seeing and other observational effects
- Non-standard cosmologies (non-isotropic, TeVeS, ...)

E- and B-modes: recap II

Measuring E- and B-modes

Separating data into E- and B-mode is not trivial.

To directly obtain $\kappa^{\rm E}$ and $\kappa^{\rm B}$ from γ, there is leakage between modes due to the finite observed field (border and mask artefacts).

One can quantify the shear pattern, e.g. with respect to reference centre points, but the tangential shear $\gamma_{\rm t}$ is not defined at the center.

Solution: filter the shear map. (= convolve with a filter function Q). This also has the advantage that the spin-2 quantity shear is transformed into a scalar.

This is equivalent to filtering κ with a function U that is related to Q.

E- and B-modes: recap III

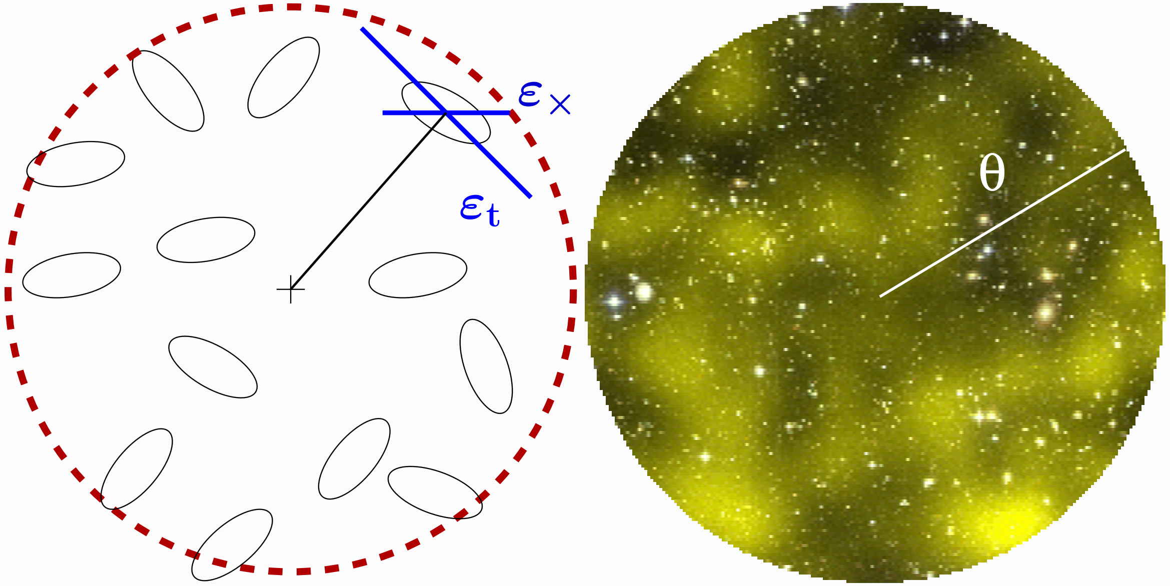

The resulting quantity is called aperture mass $M_{\rm ap}(\theta)$, which is a function of the filter size, or smoothing scale, θ. It is only sensitive to the E-mode.

If one uses the cross-component shear $\gamma_\times$ instead, the filtered quantity, $M_\times$ captures the B-mode contribution only.

End of recap from part I.

Convergence as potential field

Again convergence κ and shear γ:

$$\frac{\partial \beta_i}{\partial \theta_j} \equiv A_{ij} = \delta_{ij} - \partial_i \partial_j \psi;$$

$$A = \begin{pmatrix} 1 - \kappa - \gamma_1 & -\gamma_2 \\ -\gamma_2 & 1 - \kappa + \gamma_1 \end{pmatrix}.$$

From this, write κ and γ as second derivatives of the potential.

Convergence as potential field

Again convergence κ and shear γ:

$$\frac{\partial \beta_i}{\partial \theta_j} \equiv A_{ij} = \delta_{ij} - \partial_i \partial_j \psi;$$

$$A = \begin{pmatrix} 1 - \kappa - \gamma_1 & -\gamma_2 \\ -\gamma_2 & 1 - \kappa + \gamma_1 \end{pmatrix}.$$

From this, write κ and γ as second derivatives of the potential.

$$\kappa = \frac{1}{2} \left(\partial_1 \partial_1 + \partial_2 \partial_2 \right) \psi = \frac{1}{2} \nabla^2 \psi; \;\; \gamma_1 = \frac{1}{2} \left(\partial_1 \partial_1 - \partial_2 \partial_2 \right) \psi; \;\; \gamma_2 = \partial_1 \partial_2 \psi.$$

Convergence as potential field

Again convergence κ and shear γ:

$$\frac{\partial \beta_i}{\partial \theta_j} \equiv A_{ij} = \delta_{ij} - \partial_i \partial_j \psi;$$
$$A = \begin{pmatrix} 1-\kappa-\gamma_1 & -\gamma_2 \\ -\gamma_2 & 1-\kappa+\gamma_1 \end{pmatrix}.$$

From this, write κ and γ as second derivatives of the potential.

$$\kappa = \frac{1}{2}\left(\partial_1\partial_1 + \partial_2\partial_2\right)\psi = \frac{1}{2}\nabla^2\psi; \;\; \gamma_1 = \frac{1}{2}\left(\partial_1\partial_1 - \partial_2\partial_2\right)\psi; \;\; \gamma_2 = \partial_1\partial_2\psi.$$

We can now define a vector field $\boldsymbol{u}$ for which the convergence is the "potential", with

$$\boldsymbol{u} = \boldsymbol{\nabla}\kappa.$$

Express $\boldsymbol{u}$ in terms of the shear.

Convergence as potential field

Again convergence κ and shear γ:

$$\frac{\partial \beta_i}{\partial \theta_j} \equiv A_{ij} = \delta_{ij} - \partial_i \partial_j \psi;$$

$$A = \begin{pmatrix} 1 - \kappa - \gamma_1 & -\gamma_2 \\ -\gamma_2 & 1 - \kappa + \gamma_1 \end{pmatrix}.$$

From this, write κ and γ as second derivatives of the potential.

$$\kappa = \frac{1}{2}\left(\partial_1\partial_1 + \partial_2\partial_2\right)\psi = \frac{1}{2}\nabla^2\psi; \;\; \gamma_1 = \frac{1}{2}\left(\partial_1\partial_1 - \partial_2\partial_2\right)\psi; \;\; \gamma_2 = \partial_1\partial_2\psi.$$

We can now define a vector field $\boldsymbol{u}$ for which the convergence is the “potential”, with

$$\boldsymbol{u} = \boldsymbol{\nabla}\kappa.$$

Express $\boldsymbol{u}$ in terms of the shear.

$$\boldsymbol{u} = \begin{pmatrix} \partial_1\kappa \\ \partial_2\kappa \end{pmatrix} = \begin{pmatrix} \frac{1}{2}(\partial_1\partial_1\partial_1 + \partial_1\partial_2\partial_2)\psi \\ \frac{1}{2}(\partial_1\partial_1\partial_2 + \partial_2\partial_2\partial_2)\psi \end{pmatrix} = \begin{pmatrix} \partial_1\gamma_1 + \partial_2\gamma_2 \\ -\partial_2\gamma_1 + \partial_1\gamma_2 \end{pmatrix}.$$

E- and B-mode potential, convergence, and shear I

Thus, from a shear field γ, to linear order, the corresponding convergence is derived from a gradient field $\boldsymbol{u}$, and is curl-free, $\boldsymbol{\nabla} \times \boldsymbol{u} = \partial_1 u_2 - \partial_2 u_1 = 0$, as can easily be seen.
This is the E-mode, in analogy to the electric field.

However, in reality, from an observed shear field, one might measure a non-zero curl component.
This is called the B-mode, in analogy to the magnetic field.

Definition:

$$\nabla^2 \kappa^{\mathrm{E}} := \boldsymbol{\nabla} \cdot \boldsymbol{u};$$
$$\nabla^2 \kappa^{\mathrm{B}} := \boldsymbol{\nabla} \times \boldsymbol{u},$$

and potentials

$$\nabla^2 \psi^{\mathrm{E,B}} = 2\kappa^{\mathrm{E,B}}.$$

Note that ψ^{B} and κ^{B} do not correspond to physical mass over-densities.

Aperture mass

Earlier we have mentioned the aperture-mass. This is formally defined as convolution of the shear field with a filter Q,

$$M_{\rm ap}(\theta, \boldsymbol{\vartheta}) = \int \mathrm{d}^2\vartheta' \, Q_\theta(|\boldsymbol{\vartheta} - \boldsymbol{\vartheta}'|) \, \gamma_{\rm t}(\boldsymbol{\vartheta}')$$

It can be shown that this is equivlaent of convolving the convergence with another filter U,

$$M_{\rm ap}(\theta, \boldsymbol{\vartheta}) = \int \mathrm{d}^2\vartheta' \, U_\theta(|\boldsymbol{\vartheta} - \boldsymbol{\vartheta}'|) \, \kappa^{\rm E}(\boldsymbol{\vartheta}'), \qquad (2)$$

(Kaiser et al. 1994, Schneider 1996).

E-/B-mode separation with M_{ap} I

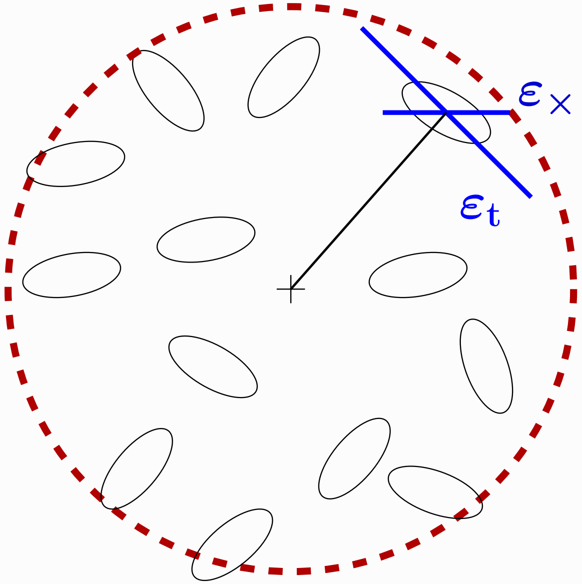

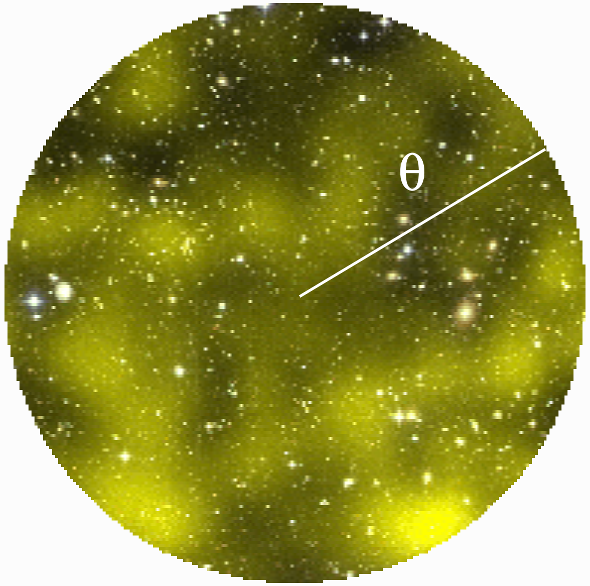

It is clear that M_{ap} ($M_\times$) is sensitive to the E-mode (B-mode) of the shear field γ.

When chosing Q such that its support is finite, with $Q(\theta) = 0$ for $\theta > \theta_{\mathrm{max}}$, the E-/B-mode separation is achieved on a finite interval.

To get this separation at the second-order level, let's take the variance of the aperture-mass: Square $M_{\mathrm{ap}}(\theta, \boldsymbol{\vartheta})$ and average over circle centres $\boldsymbol{\vartheta}$ (Schneider et al. 1998).

E-/B-mode separation with $M_{\rm ap}$ II

Square $M_{\rm ap}(\theta, \boldsymbol{\vartheta})$ and average over circle centres $\boldsymbol{\vartheta}$:

$$
\begin{aligned}
\langle M_{\rm ap}^2 \rangle(\theta) &= \int \mathrm{d}^2\vartheta' \, U_\theta(|\boldsymbol{\vartheta} - \boldsymbol{\vartheta}'|) \int \mathrm{d}^2\vartheta'' \, U_\theta(|\boldsymbol{\vartheta} - \boldsymbol{\vartheta}''|) \langle \kappa^{\rm E}(\boldsymbol{\vartheta}') \kappa^{\rm E}(\boldsymbol{\vartheta}'') \rangle \\
&= \int \mathrm{d}^2\vartheta' \, U_\theta(\vartheta') \int \mathrm{d}^2\vartheta'' \, U_\theta(\vartheta'') \langle \kappa^{\rm E} \kappa^{\rm E} \rangle (|\boldsymbol{\vartheta}' - \boldsymbol{\vartheta}''|) \\
&= \int \mathrm{d}^2\vartheta \, U_\theta(\vartheta) \int \mathrm{d}^2\vartheta' \, U_\theta(\vartheta') \\
&\quad \times \int \frac{\mathrm{d}^2\ell}{(2\pi)^2} \mathrm{e}^{-\mathrm{i}\boldsymbol{\ell}\boldsymbol{\vartheta}} \int \frac{\mathrm{d}^2\ell'}{(2\pi)^2} \mathrm{e}^{-\mathrm{i}\boldsymbol{\ell}\boldsymbol{\vartheta}'} (2\pi)^2 \delta_{\rm D}(\boldsymbol{\ell} - \boldsymbol{\ell}') P_\kappa^{\rm E}(\ell) \\
&= \int \frac{\mathrm{d}^2\ell}{(2\pi)^2} \left(\int \mathrm{d}^2\vartheta \, \mathrm{e}^{2\mathrm{i}\boldsymbol{\ell}\boldsymbol{\vartheta}} U_\theta(\vartheta) \right)^2 P_\kappa^{\rm E}(\ell) \\
&= \frac{1}{2\pi} \int \mathrm{d}\ell \, \ell \, \hat{U}^2(\theta\ell) P_\kappa^{\rm E}(\ell).
\end{aligned}
$$

Note: Typically, the filter function U depends on the scale ϑ normalized to the radius θ, $U_\theta(\vartheta) = U(\vartheta/\theta)$. In Fourier space this then becomes $\hat{U}(\theta\ell)$.

E-/B-mode separation with $M_{\rm ap}$ III

For popular choices of U, $\hat U^2$ is a narrow pass-band filter function.

	polynomial	Gaussian
$U_\theta(\vartheta)$	$\begin{cases} \frac{9}{\pi\theta^2}\left(1-\frac{\vartheta^2}{\theta^2}\right)\left(\frac{1}{3}-\frac{\vartheta^2}{\theta^2}\right) & \lvert\vartheta\rvert<\theta \\ 0 & \text{else} \end{cases}$	$\frac{1}{2\pi\theta^2}\left(1-\frac{\vartheta^2}{2\theta^2}\right)\exp\left(-\frac{\vartheta^2}{2\theta^2}\right)$
$Q_\theta(\vartheta)$	$\begin{cases} \frac{6}{\pi\theta^2}\frac{\vartheta^2}{\theta^2}\left(1-\frac{\vartheta^2}{\theta^2}\right) & \lvert\vartheta\rvert<\theta \\ 0 & \text{else} \end{cases}$	$\frac{\vartheta^2}{4\pi\theta^4}\exp\left(-\frac{\vartheta^2}{2\theta^2}\right)$
$\hat U(\eta)$	$\frac{24 \mathrm{J}_4(\eta)}{\eta^2}$	$\frac{\eta^2}{2}\exp\left(\frac{-\eta^2}{2}\right)$

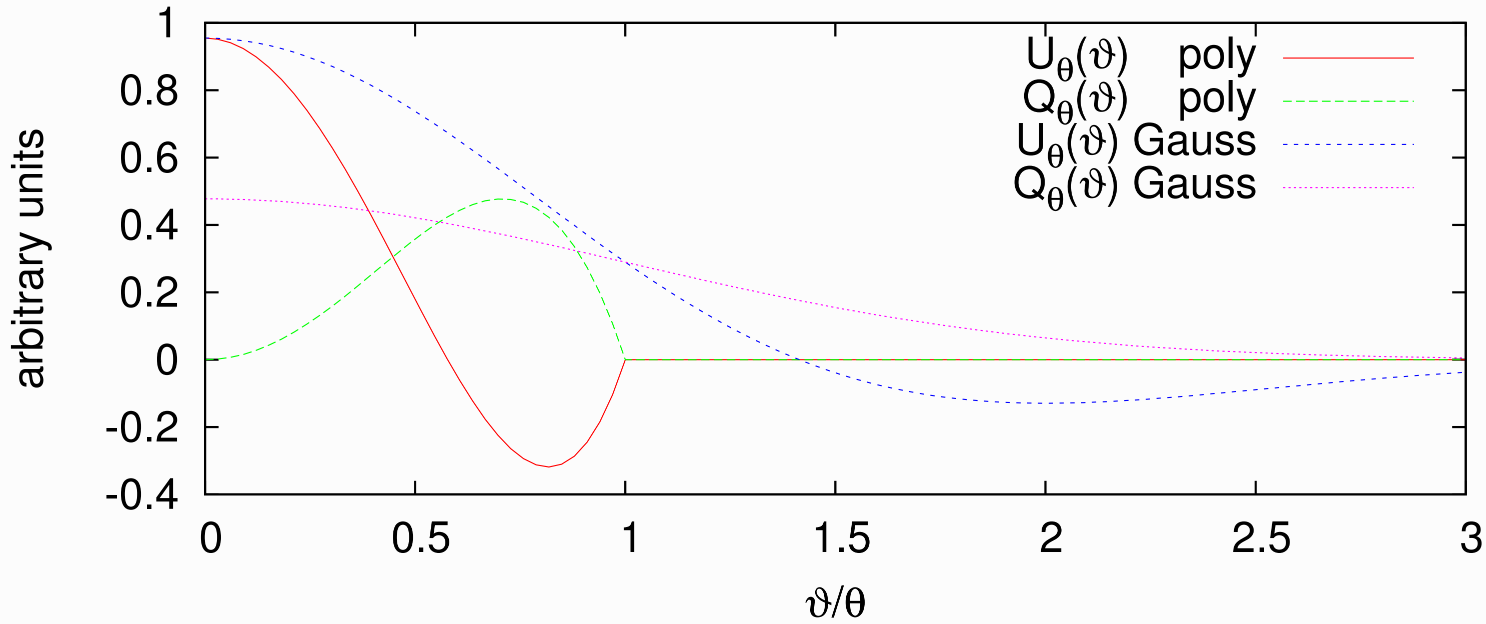

Aperture-mass dispersion measurements

CFHTLS 2007 versus CFHTlenS 2013.

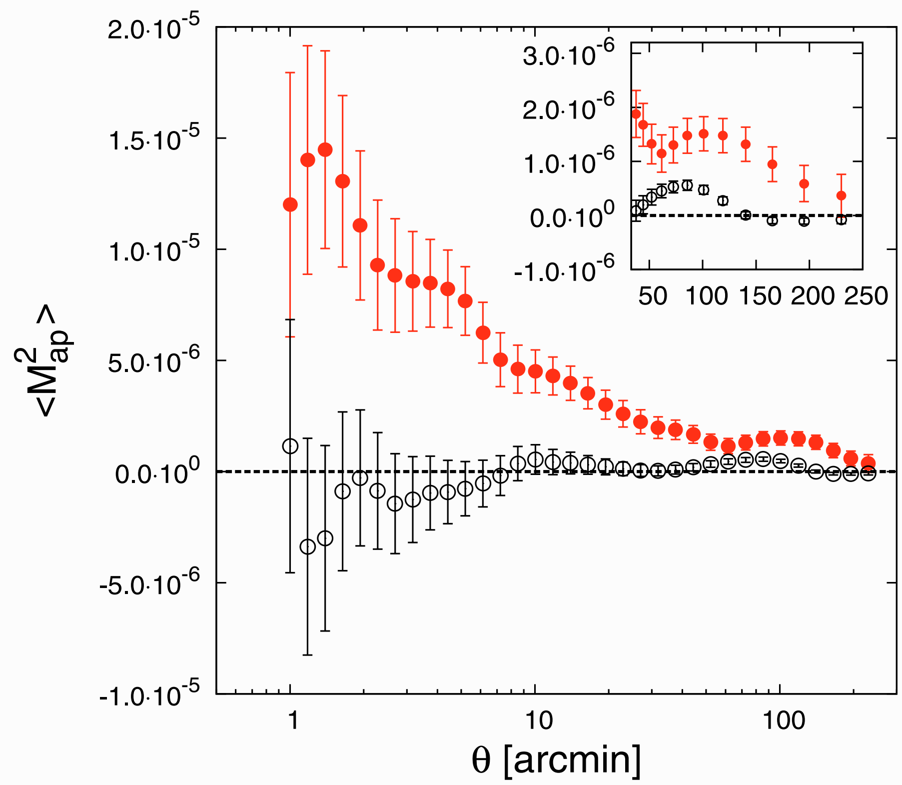

From (Fu et al. 2008).

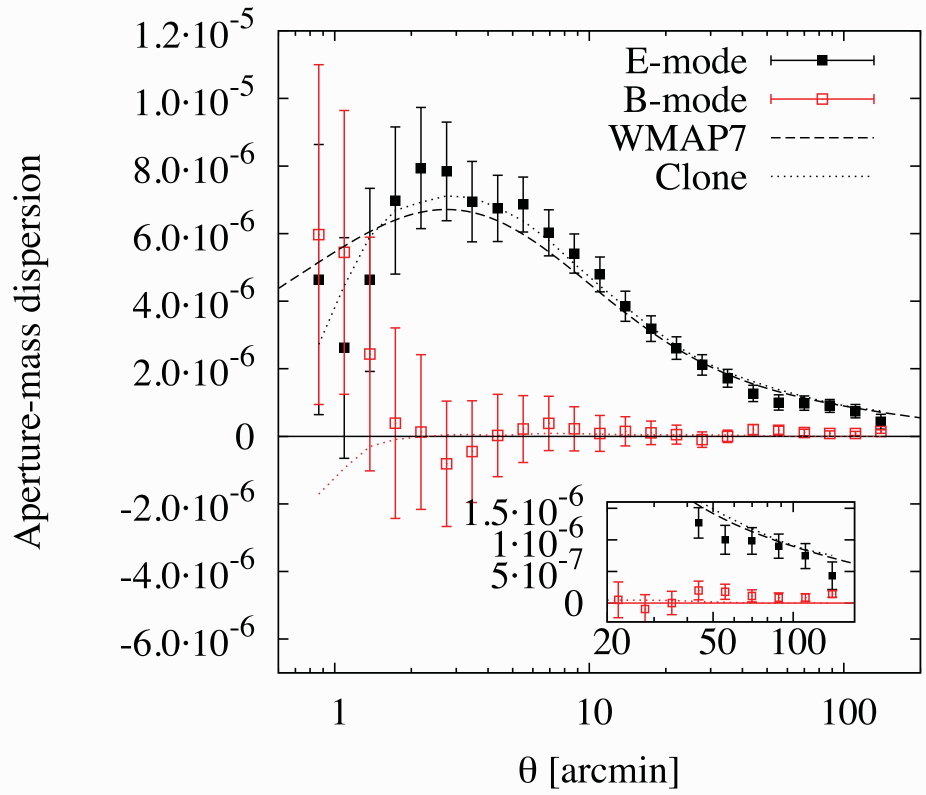

From (Kilbinger et al. 2013).

Ring statistic I

The problem of the unaccessible zero lag shear correlation for an E- and B-mode decomposition remains. How can we construct a E-/B-mode second-order correlation with a minimum galaxy separation $\vartheta_{\min} > 0$?

Solution: Correlate shear on two concentric rings (Schneider & Kilbinger 2007).
What are the minimum and maximum distances in this configuration?

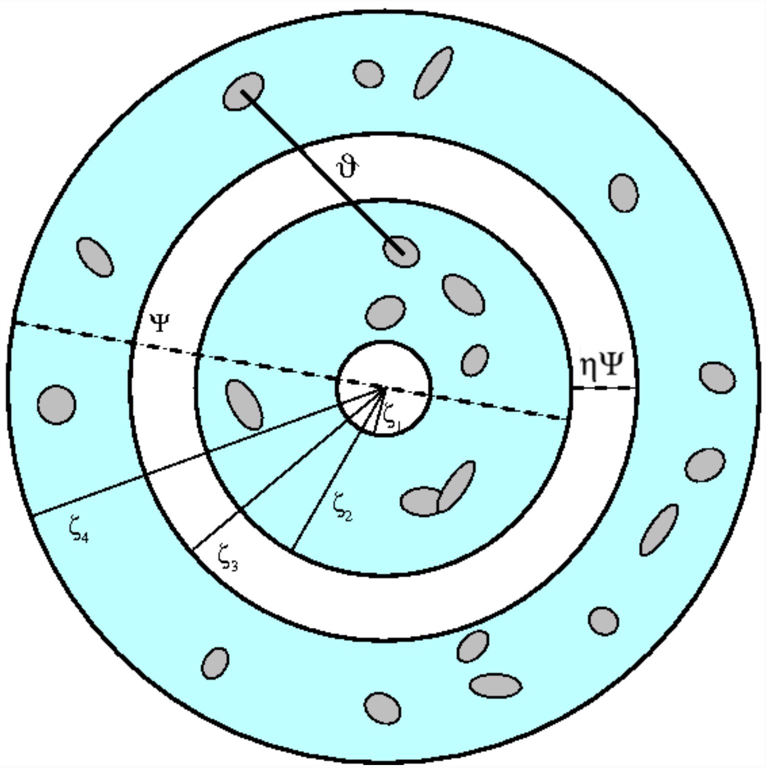

Figure from (Eifler et al. 2010).

Ring statistic measurements

CFHTLS 2007 versus CFHTLenS 2013.

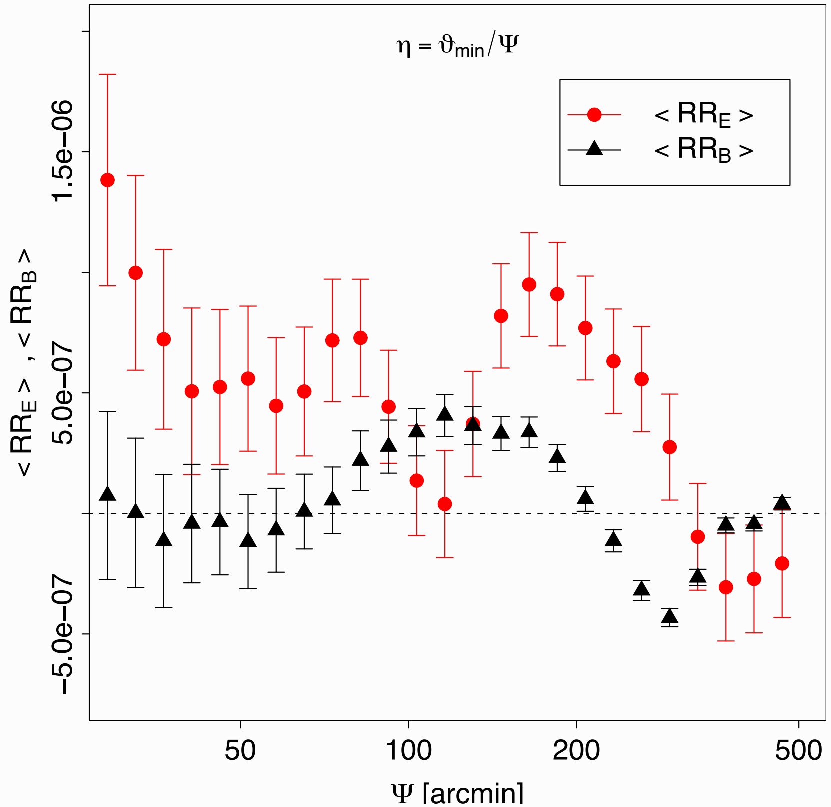

From (Eifler et al. 2010).

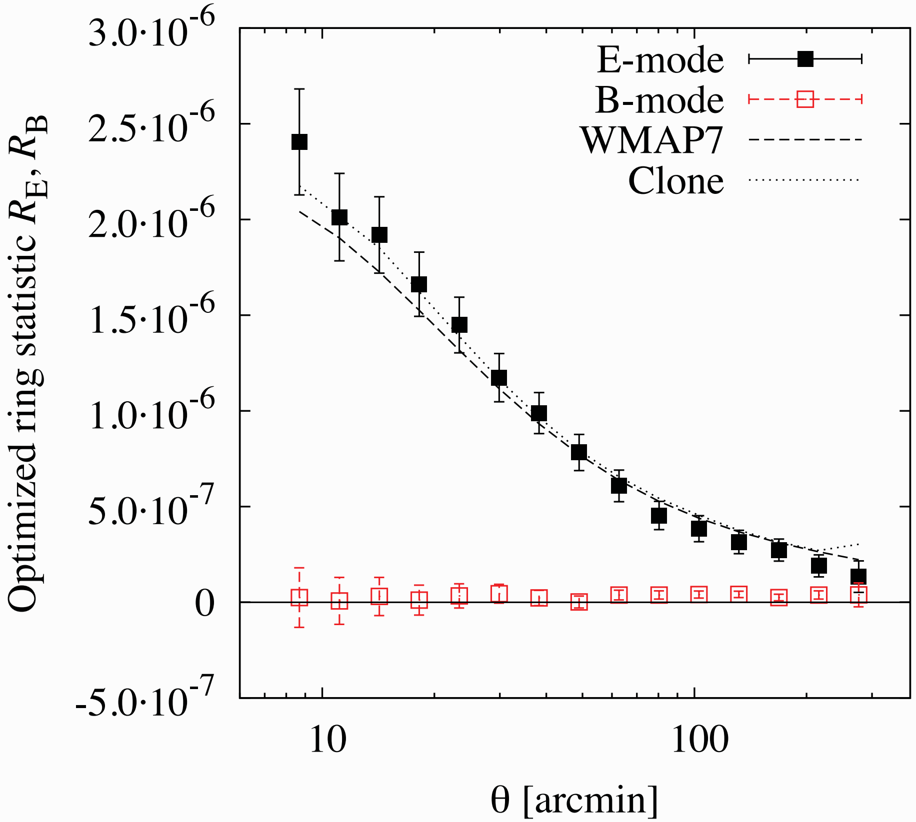

From (Kilbinger et al. 2013), optimised ring statisc following (Fu & Kilbinger 2010).